ISSN 1027-5495. Functional Materials, 28, No.2 (2021), p. 225-233.
doi:https://doi.org/10.15407/fm28.02.225

Structural and luminescent properties of the fluorine co-doped ZrO_2:Y and ZrO_2:Eu nanopowders

***V.Chornii*[1,2], *V.Boyko*[1], *S.G.Nedilko*[2], *P.Teselko*[2], *K.Terebilenko*[2], *M.Slobodyanik*[2], *V.Prokopets*[2], *V.Sheludko*[3], *O.Gomenyuk*[3]**

[1]National University of Life and Environmental Sciences of Ukraine, 15 Geroiv Oborony Str., 03041 Kyiv, Ukraine
[2]T.Shevchenko National University of Kyiv, 64/13 Volodymyrska Str., 01601 Kyiv, Ukraine
[3]O.Dovzhenko Hlukhiv National Pedagogical University, 24 Kyivo-Moskovs'ka Str., 41401 Hlukhiv, Ukraine

Received August 30, 2020

The results of calculations of the electronic band structure and experimental studies of zirconia (ZrO_2) pure and doped with fluorine, fluorine/europium and fluorine/yttrium are reported. The incorporation of fluorine into polycrystalline zirconia was achieved by solid state synthesis. The studied powders were characterized by scanning electron microscopy, powder X-ray diffraction and luminescent spectroscopy. The samples were the mixture of the monoclinic and cubic zirconia polymorphs with a particle size distribution within 50–200 nm. Under excitation with 395 nm at T = 77 K, all the samples revealed intensive wideband host luminescence attributed to the F^+ and F^0 luminescence centers. Zirconium dioxide doped with europium demonstrates a linear red emission of the Eu^{3+} ions in addition to the host photoluminescence. In the case of samples co-doped with fluorine and europium the emission intensity of the Eu^{3+} ions increased by about 8 times as compared to the ZrO_2:Eu sample. The effect of fluorine on structural and optical properties of zirconia was discussed taking into account experimental data and results of calculations.

Keywords: defect, europium, fluorine, luminescence, zirconia.

Структурні та люмінесцентні властивості нанопорошків ZrO_2:Eu та ZrO_2:Y, співлегованих фтором. *В.Чорній, В.Бойко, С.Г.Неділько, П.Теселько, К.Теребіленко, М.Слободяник, В.Прокопець, В.Шелудько, О.Гоменюк*

Наведено результати розрахунку електронної структури та експериментальних досліджень діоксиду цирконію (ZrO_2) як "чистого", так і легованого фтором і європієм та фтором і ітрієм. Введення фтору до полікристалічного діоксиду цирконію і було виконано шляхом твердофазного синтезу. Одержані порошки досліджено методами скануючої електронної мікроскопії, порошкової рентгенівської дифракції та люмінесцентної спектроскопії. Зразки є сумішшю моноклінного та кубічного цирконію з розміром частинок у межах 50–200 нм. Всі зразки при збудженні 395 нм і температурі 77 К виявляють інтенсивну широкосмугову люмінесценцію матриці, віднесену до F^+ і F^0 центрів свічення. Зразки діоксиду цирконію, леговані європієм, окрім фотолюмінесценції матриці, виявили лінійчате червоне свічення іонів Eu^{3+}. Для зразків, співлегованих фтором та європієм, інтенсивність свічення іонів Eu^{3+} зросла приблизно у 8 разів у порівнянні з випадком ZrO_2:Eu^{3+}. Вплив фтору на структуру та оптичні властивості діоксиду цирконію обговорено з експериментальними даними та результатами розрахунків.

Сообщаются результаты расчета электронной структуры и экспериментальных исследований диоксида циркония (ZrO_2) как "чистого", так и легированного фтором, фтором и европием, фтором и иттрием. Введение фтора в поликристаллический диоксид циркония выполнено путем твердофазного синтеза. Полученные порошки исследованы методами сканирующей электронной микроскопии, порошковой рентгеновской дифракции и люминесцентной спектроскопии. Образцы представляют собой смесь моноклинного и кубического циркония с размером частиц в пределах 50–200 нм. Во всех образцах при возбуждении 395 нм и температуре 77 K обнаружена интенсивная широкополосная люминесценция матрицы, приписанная F^+ и F^0 центрам свечения. Образцы диоксида циркония, легированного европием, кроме фотолюминесценции матрицы, имеют линейчатое красное свечение ионов Eu^{3+}. Для образцов, легированных фтором и европием, интенсивность свечения ионов Eu^{3+} выросла примерно в 8 раз в сравнении с образцом ZrO_2:Eu^{3+}. Влияние фтора на структуру и оптические свойства диоксида циркония обсуждаются с экспериментальными данными и результатами расчетов.

1. Introduction

Energy efficiency of the devices is one of the key problems of modern engineering that determines the main trends in materials science. Recently, great attention has been paid to elaboration of phosphor-converting white light emitting diodes (pc-WLED) as energy effective devices for solid-state lighting and display applications [1, 2]. Important component of the pc-WLED is a phosphor, which must have high luminescence intensity and at the same time be resistant to water, temperature variation, intensive light fluxes, etc. All the mentioned conditions are satisfied by oxide compounds doped with rare-earth (RE) ions. Zirconia (zirconium dioxide, ZrO_2) has been intensively studied among oxide phosphors as a multifunctional material with good physical properties, in particular, luminescent ones [3–5]. It is known that ZrO_2 reveals intrinsic host photoluminescence (PL) in the visible spectral range and up to eight bands can be distinguished in emission spectra of un-doped zirconia [6]. These PL bands of zirconia have been attributed to so-called *F*-centers (e.g. F^0, F^+ and F_2) centers formed at oxygen vacancies [7–10]. Doping with Eu^{3+} ions improves the luminescence properties of polycrystalline ZrO_2 as red phosphor for WLED applications [11]. Eu^{3+} ions replace zirconium cations in the lattice and affect the structure and properties of ZrO_2. Consequently, intensity of the Eu^{3+} luminescence in the zirconia host depends on various factors: type of the crystalline phase, size of crystallites, dopants concentration, temperature, etc. [12–15]. It is important to note that the substitution in the anionic sublattice of zirconium dioxide is less studied than in the cationic one. The majority of studies of anion-substituted luminescent oxide materials have been devoted to doping with nitrogen leading to the formation of oxynitrides [16–20]. Among other examples of anionic substitution there are few reports dealing with the effect of chlorine and sulfur on luminescence properties of zirconia [21, 22]. As for the fluorine effect on luminescence of oxides, the majority of reports have been focused on oxyfluorides, where fluorine ions are located in regular sites within the crystal structure (e.g. [23, 24]).

Recently, it has been shown that co-doping with europium and fluorine significantly improves characteristics of red luminescence of the Eu^{3+} ions in nanocrystalline zirconia [25]. The highest PL intensity was observed for the samples doped with 0.5 mol. % of Eu^{3+} and co-doped with 8 % of fluorine. Various mechanisms have been discussed as possible reasons of the effects noted above, but due to the lack of experimental and theoretical data the mechanisms of fluorine the on influence luminescence of Eu^{3+} ions in ZrO_2:Eu,F compounds have not yet been clarified. It is important to note that the Eu^{3+} as well as Y^{3+} ions occupy Zr^{4+} positions in zirconia host by the aliovalent substitution mechanism. The difference in the charge and radius between these ions and Zr^{4+} ions leads to the formation of oxygen vacancies in the ZrO_2 lattice. There are some assumptions about the role of oxygen vacancies and the effect of fluorine doping on the luminescence centers formed on their basis [25] which require refinement and confirmation on the basis of experimental data.

The aim of this study is to investigate the effect of a fluorine dopant both on electronic and lattice structures on the basis of luminescence properties un-doped (ZrO_2:Eu) and Eu^{3+} doped zirconia (ZrO_2:Eu). Samples of zirconium dioxide doped with yttrium and fluorine (ZrO_2:F/Y) were studied as

model objects in which the triply charged dopant Y^{3+} does not participate directly in optical processes, but, as in the case of Eu^{3+}, promotes the formation of oxygen vacancies and, as a consequence, causes some structural changes in the crystal lattice of zirconium dioxide. Luminescent properties were measured for the samples cooled to a temperature of 77 K. It is known that a decrease in temperature leads to a decrease in the electron-vibration interaction in the luminescence centers and the transfer of excitation energy between them. These processes could significantly change the results and conclusions in comparison with our previous work [25], where the samples were kept at room temperature.

2. Experimental

A set of samples with the following nominal compositions: pure ZrO_2, ZrO_2:8 %F (hereafter denoted as Zr(0) and Zr(F), respectively), ZrO_2:0.5 %Eu (denoted as Zr(Eu)), ZrO_2:0.5 %Eu/8 %F (denoted as Zr(F/Eu) and ZrO_2:8 %F/2 %Y (denoted as Zr(F/Y) was obtained by a solid state method under the same synthesis conditions. The details of preparation of Zr(Eu) and Zr(F/Eu) ceramics can be found in [25]. The samples of Zr(0), Zr(F) and Zr(F/Y) were synthesized in the following way. A stoichiometric mixture of $ZrO(NO_3)_2 \cdot 2H_2O$, Y_2O_3, and ZrF_4 was calcined at 723 K to decompose the first ingredient, and then gradually heated to 973, 1073, 1173, and 1273 K, holding for 6 h at each temperature with intermediate grinding. The final products were white polycrystalline powders. The X-ray powder diffraction was used to check the phase composition of the prepared samples. X-ray diffraction patterns were obtained using a conventional powder diffractometer Siemens D500 operating in Bragg-Brentano ($\theta/2\theta$) geometry using a Ni β-filter in CuK_α radiation.

Scanning electron-microscopic (SEM) images of the powders coated with gold were obtained at a JEOL JSM 6060 LV instrument; these images were used to analyze morphology and sizes of the crystalline particles of the samples.

The electronic structure of the crystals was analyzed using theoretical calculations made with the WIEN2k program package [26], in which the method of full-potential linear-augmented-plane-wave was implemented within the framework of density functional theory (DFT). The crystal structure parameters reported in [27] were used for calculation of the electronic band structure of perfect monoclinic zirconia. Calculations for monoclinic zirconia doped with fluorine, fluorine-europium and fluorine-yttrium were performed in the super-cell approach, using of 2 cells along the x direction (this super-cell contains 8 zirconium atoms and 16 oxygen atoms). In the case of a single fluorine impurity, one oxygen atom in the regular site was replaced by fluorine and the system under study can be named $Zr_8O_{15}F$. The zirconium atom was replaced by either a europium or yttrium atom for the case of a crystal with fluorine- europium and fluorine-yttrium dopants. Calculations of the electronic band structure were performed for geometry optimized supercells. The energy band gap values for all the calculations are underestimated, that is a property of DTF calculations [28], but we decided to present the partial densities of electronic states (PDOS) as they have been obtained, without any correction, since this problem is not very important for this study.

The specific features of the transitions of excitation and emission were revealed from the spectral data of photoluminescence and luminescence excitation. The PL study of the samples at a temperature of 77 K was carried out under excitations by the light of UV and visible ranges using a DFS-12 spectral complex. An arc Xenon lamp (1500 W) was used together with a DMR-4 monochromator as an exciting light source. All the spectra were corrected according to the response of the registering system.

3. Results and discussion

Our earlier study has shown that ZrO_2:0.5 %Eu/8 %F reveals the most intensive luminescence among ZrO_2:0.5 %Eu/xF samples [25]. It is known, that an increase in the amounts of both Eu_2O_3 and Y_2O_3 increases the contribution of the highly symmetric zirconia crystal phase in comparison to monoclinic one, but the amount of the highly symmetric phase increases more significantly for the case of the Eu_2O_3 dopant. For instance, ZrO_2 doped with 2 mol. % of Eu_2O_3 contains a tetragonal phase fraction of about 30 % with an average grain size of 0.35 μm [29], while for ZrO_2 doped with Y_2O_3, the same tetragonal phase content is obtained for ZrO_2 doped with 3 mol. % of Y_2O_3. The average grain size is about 0.5 μm for the composition discussed above [30]. For the samples under study, the combined substitution with fluorine and yttrium oxide has a similar effect

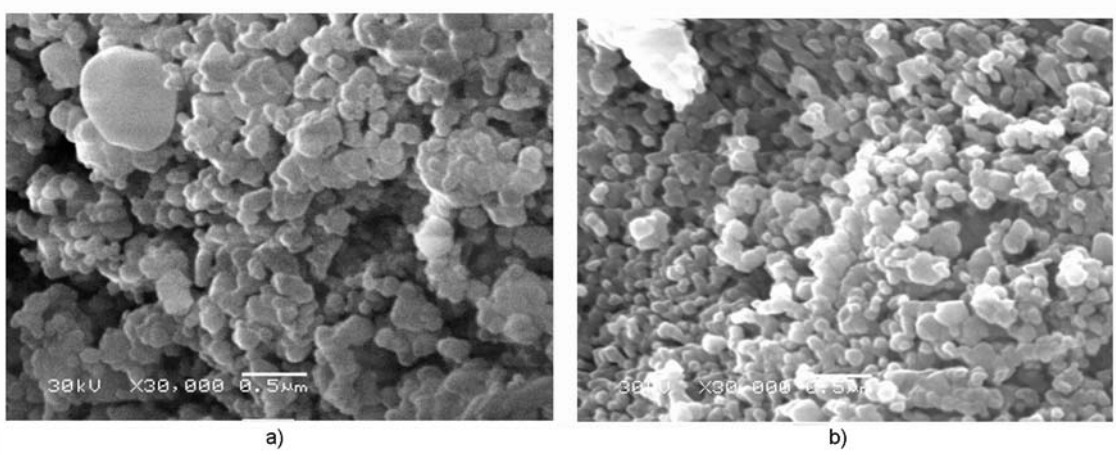

Fig. 1. SEM images of Zr(F/Y) (a) and Zr(F/Eu) samples (b).

on morphology, shape and particle size in the case of samples ZrO_2:0.5 %Eu/8 %F and ZrO_2:2 %Y 8 %F (denoted above as Zr(F/Y).

In fact, the results of SEM measurements showed that Zr(F,Eu) and Zr(F/Y) powders consist of agglomerates of nanosized particles with the same shape and sizes for both compositions (Fig. 3). The particle size distribution ranges from 50 to 200 nm both for Zr(F/Eu) and Zr(F/Y) (Fig. 1).

The results of the XRD study confirm an assumption about the phase composition. The XRD patterns for all studied samples and standards for monoclinic and cubic zirconia are shown in the Fig. 2. It is known that highly symmetric tetragonal and cubic zirconia structures are similar providing the same XRD patterns. Therefore, only one standard is used in Fig. 2 for comparison with experimental patterns.

It can be seen that Zr(0) and Zr(F) samples are pure monoclinic phases of zirconia (Fig. 2, curves *1* and *2*). The europium- and yttrium-containing samples (Zr(F/Eu)) and Zr(F/Y) are mixtures of monoclinic and cubic phases with the similar ratio of the phases (Fig. 2, curves 3 and 4). It is known that the size of the particles plays an important role in phase stabilization. Moreover, the size of particles affects zirconia polymorphs properties [31, 32]. In particular, monoclinic zirconia is not stable in the form of nanoparticles if the crystallite sizes are below of 9–20 nm [32]. In order to estimate the minimal grain sizes of the samples under study, the well-known Scherrer formula was applied to analyze the XRD data. Thus, the XRD peaks at $2\Theta = 28.3$, 30.3 and 31.6 deg were used for the calculations. It was found that the smallest grains of

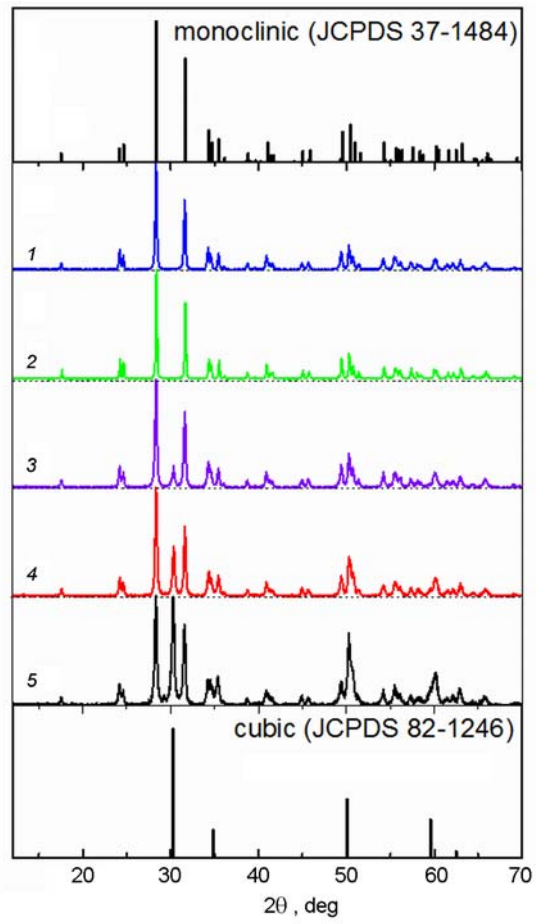

Fig. 2. XRD patterns of the ZrO_2 (*1*), Zr(F) (*2*), Zr(Eu) (*3*), Zr(F/Y) (*4*) and Zr(F/Eu) (*5*) samples. Standards for monoclinic and cubic zirconia are shown at the top and at the bottom of the figure, respectively.

cubic zirconia (calculated for XRD peak at 30.3 deg) in both samples Zr(F/Y) and Zr(F/Eu) have size near 27 nm. The smallest grains of F/monoclinic zirconia in Zr(F/Y)

and Zr(F/Eu) samples have sizes 34 and 27 nm, respectively. The obtained size values are quite close to each other, that confirms the similarity of the structural properties of the Zr(F/Y) and Zr(F/Eu) patterns.

The effect of RE and fluorine dopants on the zirconia electronic structure was calculated theoretically. For comparative analysis, also the electronic band structure of perfect zirconia was calculated. The results of calculations of the partial density of electronic states (PDOS) are shown in the Fig. 3 only in the energy range from –6 to 12 eV for the electronic states of a significant partial density. The origin of the energy scale was chosen at the top of the valence band. The positions of the Fermi level are shown in Fig. 3 for each of the calculated compositions.

The calculated PDOS curves showed that the valence band top is mainly formed by O *p* states and the conduction band bottom is mainly formed by Zr *d* states for all the studied compositions. The results of the calculations for perfect monoclinic zirconia and doped with fluorine zirconia are in good agreement with data of previous works [33–36]. The states of the fluorine are mostly located at the deep part of the valence band for all fluorine doped structures under study. Yttrium impurity states are represented by *d* states which are in the upper parts of the conduction band in the electronic structure of fluorine containing zirconia. So, there are no defect levels in the band gap of both zirconia doped with fluorine and zirconia co-doped with yttrium and fluorine.

As for zirconia crystals doped with europium ions, their electronic structure is represented by partially occupied Eu *f* states located near the middle of the band gap and by the un-occupied Eu *d* states in the upper part of the conduction band of fluorine-containing zirconium dioxide. Therefore, as in the case of the Zr8Y crystal, the electronic structure of the Zr8Eu crystals doped with fluorine does not have levels of any other defects in the band gap.

The absence of any additional defect levels in the band gap of fluorine/yttrium and fluorine/europium co-doped zirconia indicates that the incorporation of fluorine in this basic material does not create additional channels for the excitation energy losses. Therefore, we believe that the main effect of doping with fluorine on zirconia is the suppression of the number of oxygen vacancies. It should be noted that this conclusion is based on a rough approximation

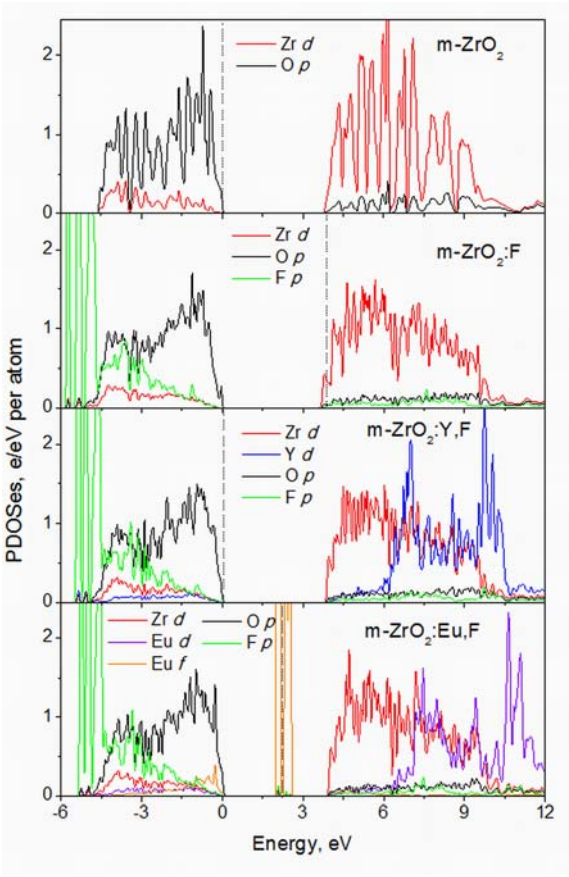

Fig. 3. PDOS of the monoclinic zirconia calculated for regular and doped zirconia crystals. The Fermi levels are also shown by vertical dot lines.

when the data of the calculation of the electronic band structure of bulk monoclinic zirconium dioxide were used for the analysis. It would be very important to carry out calculations in cluster approximations for nanoparticles of zirconia polymorphs with variety of defects including oxygen vacancies, fluorine, yttrium and europium ions, as well as their combinations.

It is known from the results of previous studies that the presence of oxygen vacancies is revealed in the spectra of intrinsic luminescence of un-doped and doped zirconia. To confirm this statement, the luminescent properties of the samples under study were analyzed. The photoluminescence spectra of the samples are shown in the Fig. 4.

In the case of un-doped zirconia (Zr(0) sample), a wide complex PL band with the main maximum near 450 was observed. The high-energy part of the spectrum can be described by three Gaussian curves with maxima at 2.90, 2.71, and 2.51 eV, which contain about 88 % of the total PL intensity. The main contribution from them (68 %)

falls on the component at 2.51 eV, while the other two (2.71 and 2.90 eV) components give 15 and 17 % contributions, respectively. The Gaussian component at 2.06 eV describes a low energy part of the spectra and it gives 12 % of the total PL intensity. According to the published data on the luminescence of zirconia, the noted high-energy PL components (2.51, 2.71, and 2.9) can be associated with oxygen vacancies (various types of F centers) [7–9, 37]. In particular, it was suggested that the PL bands of zirconium dioxide in the range of 2.8–3.0 eV are responsible for the F^+ centers [38–40].The band at ~ 2.4 eV observed in [41] was assigned to F^0 center, while the low energy and low PL emission intensity can be caused by uncontrolled Ti and Hf impurities or some other local defects of very low concentration [42, 43].

The doping of zirconia with fluorine ions results in a decrease in the luminescence intensity over the entire spectrum of emission. In this case, the maxima of the PL bands are red-shifted up to 460 nm. Undoubtedly, this is due to the redistribution of contributions of various PL components in the total spectrum. In fact, the spectrum of the Zr(F) sample is fitted by only two high-energy Gaussian curves with maxima at 2.71 (2 % of total intensity) and 2.51 eV (87 % of the total intensity). There is also a low-energy component that spreads over a wide spectral range and accounts for 11 % of the total intensity. So, we can state that the 2.9 eV component disappears, the contribution of the 2.71 component decreases, while the contribution of the 2.51 band increases for the sample Zr(F) in comparison with the spectrum for the Zr(0) sample.

The total luminescence intensity of the host increased almost twofold for the samples doped with europium ions as compared with the data for the undoped sample. (Fig. 4, curve *3*). An increase in the intensity of the total emission should be associated with an increase in the number of oxygen vacancies due to the partial replacement of Zr^{4+} ions by Eu^{3+} ions [11, 13, 15]. At the same time, we found that the 2.51 eV band contributes 77 % intensity, while the contributions of the bands at 2.71 and 2.90 eV are near zero and 6 %, respectively. The noted redistribution of the intensity components shows that the ratio of the various types of oxygen vacancies associated with PL centers also changes after doping with Eu^{3+} ions. Some increase in the long-wavelength part of the PL spectra for the Zr(Eu) samples

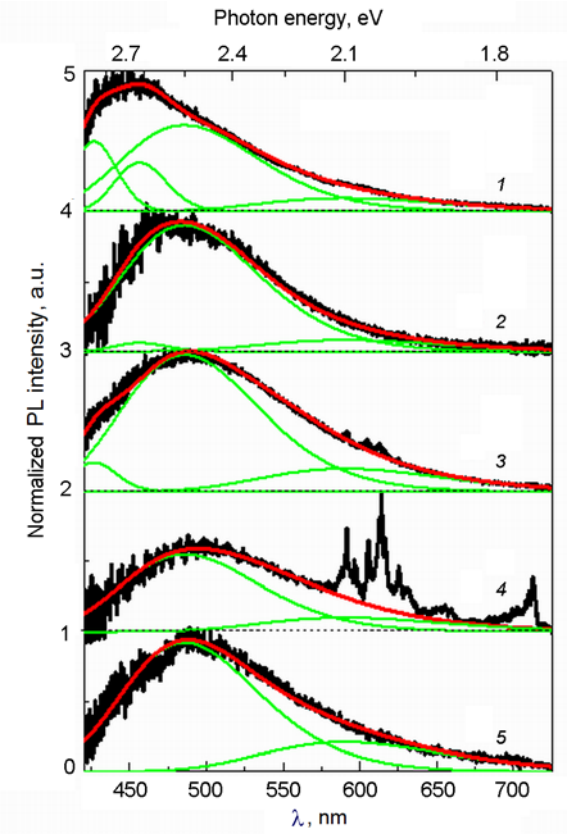

Fig. 4. PL spectra of the Zr(0) (*1*), Zr(F) (*2*), Zr(Eu) (*3*), Zr(F/Eu) (*4*) and Zr(F/Y) (*5*) samples; λ_{ex} = 395 nm; T = 77 K. Zero intensity levels for the *1–4* spectra are shown by dashed lines, Gaussian curves — by green lines and Gaussian curves sums are shown by red lines.

should be associated with defects caused by the zirconium lattice deformations due to the above noted $Zr^{4+} \rightarrow Eu^{3+}$ substitution.

Low intensity details in the 585–635 nm spectral range were also observed for the Zr(Eu) samples and they should be attributed to *f–f* transitions in the inner shell of the Eu^{3+} ions [3, 13, 25]. The emission intensity of Eu^{3+} increases sharply (by about 8 times), if Eu^{3+} ions are incorporated into the samples additionally doped with fluorine — Zr(F/Eu) (Fig. 4, curve *4*). In addition, for such samples, a decrease in the total intensity of host luminescence to a level characteristic of Zr(F) samples was observed.

The changes in the luminescence characteristics of the Zr(F/Y) samples compared to the Zr(0) samples are the result of the combined action of F^- ions and three-charged Y^{3+} ions similarly to the situation described above. We have found that the emission from Zr(F/Y) samples gives only a wide band

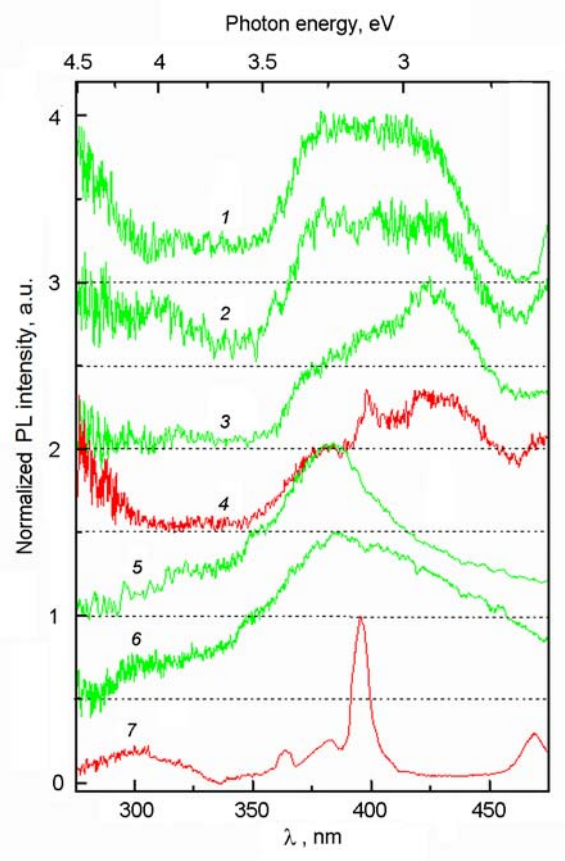

Fig. 5. PL excitation spectra of Zr(0) (*1*), Zr(F) (*2*), Zr(Eu) (*3*, *4*), Zr(F/Y) (*5*) and Zr(F/Eu) samples (*6*, *7*) registered at λ_{em} = 500 (*1–3*, *5*, *6*), and 613 nm (*4*, *7*); T = 77 K. Zero intensity levels for the 1–6 spectra are shown by dashed lines.

at the short wavelength side and a wide band at the long wavelength side of the spectrum. Their shape and intensity are similar to the case of the Zr(F/Eu) sample. However, in contrast to the case of Zr(F/Eu) samples, this spectrum is not distorted due to the contribution of the emission of Eu^{3+} ions.

Therefore, the decomposition of the host-related luminescence PL spectra into Gaussian curves and a general form of the spectra allowed us to assume that fluorine ions suppress short-wavelength emission of zirconia by reducing the number of oxygen vacancies. The predominant decrease in the contribution of 2.9 and 2.71 eV bands can be associated with the transformation of the F^+ centers into another type of centers, for example, F^0.

The changes in the PL spectra described above and the assumptions about the role of the defects are consistent with data on the luminescence excitation spectra (Fig. 5). It is known that the ZrO_2 band gap width was evaluated at 4.2–6.1 eV (295–203 nm) [44]. Thus, only the short wavelength part of the excitation spectra (275–300 nm) can be caused by the allowed band-to-band absorption transitions in zirconia, while the main host-related PL band (2.51 eV) was effectively excited in the 350–450 nm spectral range and this excitation range lies out of the band-to-band transitions in ZrO_2.

The PL excitation band in the 350–450 nm range has at least two overlapping components with maxima near 380 nm (3.26 eV) and 420 nm (2.95 eV). The excitation intensity for the sample Zr(F) in general is lower than for the undoped Zr(0) sample, and some changes occur in the 300–350 nm range for fluorine-doped zirconia in comparison with undoped zirconia (curves *1* and *2* in Fig. 5). These features coincide with the described above PL results and mean that the doping with fluorine suppresses the total amount of oxygen vacancies and causes some redistribution of the centers associated with the short-wavelength PL bands (2.9 and 2.71 eV).

The doping with europium ions leads to an increase in the excitation spectrum intensity. Besides, the intensity of the 420 nm component increases in comparison with that of the 380 nm component (Fig. 5, curves 3). At the same time, it is the latter component that dominates in the excitation spectra of the host luminescence of the Zr(F/Eu) and Zr(F/Y) samples doped with fluorine (Fig. 5, curves *5* and *6*). In the PL spectra registered in the range of intrinsic Eu^{3+} luminescence (λ_{reg} = 613 nm), an additional detail occurred near 400 nm (Fig. 5, curve *4*). It is a well known peak caused by the $^7F_0 \rightarrow {}^5L_6$ absorption transition in the f shell of the Eu^{3+} ions [25]. The emission excitation spectra of Eu^{3+} ions in the Zr(F/Eu) sample confirmed this assumption, since many spectral details became available there (Fig. 5, curve *7*). These details correspond to the well-known luminescence excitation spectra of the Eu^{3+} ions [25] and it is important to point out that the intensity of this spectrum is higher than for the spectrum of the Zr(Eu) sample in which fluorine was absent. The data on PL emission and excitation showed that the host- and Eu^{3+}-associated luminescence is simultaneously and effectively excited in the same spectral range from 290 up to 475 nm. Thus, the energy of each photon absorbed by the material can be transferred to the centers associated with the host or to the Eu^{3+} ions. So, an increase in the luminescence intensity of Eu^{3+} ions can be realized

via decreasing the host luminescence intensity. Doping with fluorine contributes to this process, since fluorine ions incorporated in zirconia decrease the amount of oxygen vacancies.

At present, the literature data and our own experimental data, as well as the results of computational studies, are insufficient to establish a clear relationship between the type of defects and the bands of the host zirconia PL. Therefore, we plan to carry out a series of additional experiments, in particular, to study the effect of annealing on oxidizing and reducing arrangement for co-doped zirconia. It would be important to perform calculations in cluster approximations for zirconia nanoparticles containing many defects including oxygen vacancies, fluorine and europium ions, and their combinations.

4. Conclusions

The effect of aliovalent substitution of zirconium cations (Zr^{4+}) and oxygen anions (O^{2-}) by fluorine anions (F^{-}) and Eu^{3+} (or Y^{3+}) cations in the zirconia (ZrO_2) lattice on its structural and luminescent properties has been studied by theoretical and experimental methods.

The results of electronic band structure calculations for ideal ZrO_2, fluorine doped $ZrO_2(F)$, europium doped $ZrO_2(Eu^{3+})$, fluorine/europium co-doped $ZrO_2(F/Eu)$ and fluorine/yttrium $ZrO_2(F/Y)$ co-doped zirconia crystals showed that fluorine does not participate directly in optical absorption and emission transitions in these materials.

It was found that fluorine ions reduce the amount of oxygen vacancies in the zirconia matrix that results in a decrease in the zirconia host emission; this contributes to a sharp increase (8 times) in the luminescence intensity of Eu^{3+} ions in co-doped zirconia $ZrO_2(F/Eu)$ compared with the luminescence intensity of Eu^{3+} ions in zirconia undoped with fluorine ions.

We believe that co-doping by replacing lattice ions simultaneously in the cationic and anionic sublattices is an excellent way to improve the luminescence characteristics of rare-earth ions in oxide crystals. At the same time, we believe that further study on this issue is needed in the future to confirm this conclusion.

References

1. G.Li, Y.Tian, J.Lin, *Chem. Soc. Rev.*, **44**, 8688 (2015).
2. C.C.Lin, A.Meijerink, R.S.Liu, *J. Phys. Chem. Lett.*, **7**, 495 (2016).
3. S.D.Meetei, S.D.Singh, N.S.Singh et al., *J. Luminescence*, **132**, 537 (2012).
4. I.Ahemen, F.B.Dejene, *J. Nanopart. Res.*, **19**, 6 (2017).
5. C.Zhang, C.Li, J.Yang et al., *Langmuir*, **25**, 7078 (2009).
6. K.Hachiya, H.Oku, J.Kondoh, *Phys. Rev. B*, **71**, 064111 (2005).
7. K.Smits, L.Grigorjeva, W.Lojkowski, J.D.Fidelus, *Phys. Stat. Solidi C*, **4**, 770 (2007).
8. Y.Cong, B.Li, S.Yue et al., *J. Phys. Chem. C*, **113**, 13974 (2009).
9. K.Smits, L.Grigorjeva, D.Millers et al., *J. Luminescence*, **131**, 2058 (2011).
10. S.E.Paje, J.Llopis, *Appl. Phys. A*, **55**, 523 (1992).
11. Y.S.Vidya, K.S.Anantharaju, H.Nagabhushana et al., *Spectrochim. Acta A*, **135**, 241 (2015).
12. K.Smits, L.Grigorjeva, D.Millers et al., *Opt. Mater.*, **32**, 827 (2010).
13. L.Li, H.K.Yang, B.K.Moon et al., *J. Nanosci. Nanotechnol.*, **11**, 350 (2011).
14. I.Prochazka, J.Cizek, O.Melikhova et al., *Acta Phys. Pol. A*, **125**, 760 (2014).
15. M.A.Borik, T.V.Volkova, E.E. Lomonova et al., *Opt. Spectrosc.*, **122**, 580 (2017).
16. S.Gutzov, M.Kohls, M.Lerch, *J. Phys. Chem. Solids*, **61**, 1301 (2000).
17. S.Gutzov, M.Lerch, *Opt. Mater.*, **24**, 547 (2003).
18. F.Stavale, L.Pascua, N.Nilius, H.J.Freund, *J. Phys. Chem. C*, **118**, 13693 (2014).
19. A.Fuertes, *Mater. Horizons*, **2**, 453 (2015).
20. T.Takeda, R.J.Xie, T.Suehiro, N.Hirosaki, *Prog. Solid State Chem.*, **51**, 41 (2017).
21. M.Garcia-Hipolito, C.Falcony, M.A.Aguilar-Frutis, J.Azorin-Nieto, *Appl. Phys. Lett.*, **79**, 4369 (2001).
22. J.Chen, Z.Feng, J.Shi et al., *Chem. Phys. Lett.*, **401**, 104 (2005).
23. U.J.Gibson, K.D.Cornett, *Opt. Lett.*, **20**, 2201 (1995).
24. S.Park, T.Vogt, *J. Luminescence.* **129**, 952 (2009)
25. V.Chornii, S.G.Nedilko, M.Miroshnichenko et al., *Mater. Res. Bull.*, **90**, 237 (2017).
26. P.Blaha, K.Schwarz, G.Madsen et al., WIEN2k, Wien, Austria (2001).
27. C.J.Howard, R.J.Hill, B.E.Reichert, *Acta Crystallogr. B*, **44**, 116 (1988).
28. Y.A.Hizhnyi, S.G.Nedilko, V.P.Chornii et al., *J. Alloys Compd.*, **614**, 420 (2014).
29. S.Maschio, B.Linda, S.Bruckner, G.Pezzotti, *J. Ceram. Soc. Japan*, **108**, 593 (2000).
30. T.Sato, M.Shimada, *J. Am. Ceram. Soc.*, **67**, C-212 (1984).
31. R.C.Garvie, *J. Phys. Chem.*, **69**, 1238 (1965).
32. T.Chraska, A.H.King, C.C.Berndt, *Mater. Sci. Eng. A*, **286**, 169 (2000).

33. S.K.Pandey, *J. Phys: Condens. Matter*, **24**, 335801 (2012).
34. F.Zandiehnadem, R.A.Murray, W.Y.Ching, *Physica B+C*, **150**, 19 (1988).
35. H.Jiang, R.I.Gomez-Abal, P.Rinke, M.Scheffler, *Phys. Rev. B*, **81**, 085119 (2010).
36. J.Li, S.Meng, J.Niu, H.Lu, *J. Adv. Ceram.*, **6**, 43 (2017).
37. T.V.Perevalov, D.R.Islamov, *Microelectron. Eng.*, **178**, 275 (2017).
38. D.Nagle, V.R.PaiVerneker, A.N.Petelin, G.Groff, *Mat. Res. Bull.*, **24**, 619 (1989).
39. N.Korsunska, V.Papusha, O.Kolomys et al., *Phys. Stat. Solidi C*, **11**, 1417 (2014).
40. E.Aleksanyan, M.Kirm, E.Feldbach, V.Harutyunyan, *Radiat. Meas.*, **90**, 84 (2016).
41. C.Imparato, M.Fantauzzi, C.Passiu et al., *J. Phys. Chem. C*, **123**, 11581 (2019).
42. J.M.Carvalho, L.C.Rodrigues, J.Holsa et al., *Opt. Mater. Express*, **2**, 331 (2012).
43. R.Espinoza-Gonzalez, E.Mosquera, I.Moglia et al., *Ceram. Int.*, **40**, 15577 (2014).
44. D.W. McComb, *Phys. Rev. B*, **54**, 7094 (1996).